Environmental Science & Technology

pubs.acs.org/est

Article

Arsenic Reduces Methane Emissions from Paddy Soils: Insights from Continental Investigation and Laboratory Incubations

Ou-Yuan Jiang,[‖] Si-Yu Zhang,[‖] Xin-Di Zhao, Zi-Teng Liu, Andreas Kappler, Jian-Ming Xu, and Xian-Jin Tang*

Cite This: *Environ. Sci. Technol.* 2024, 58, 17685−17694

Read Online

ACCESS | Metrics & More | Article Recommendations | Supporting Information

ABSTRACT: Arsenic (As) contamination and methane (CH_4) emissions co-occur in rice paddies. However, how As impacts CH_4 production, oxidation, and emission dynamics is unknown. Here, we investigated the abundances and activities of CH_4-cycling microbes from 132 paddy soils with different As concentrations across continental China using metagenomics and the reverse transcription polymerase chain reaction. Our results revealed that As was a crucial factor affecting the abundance and distribution patterns of the *mcrA* gene, which is responsible for CH_4 production and anaerobic CH_4 oxidation. Laboratory incubation experiments showed that adding 30 mg kg^{-1} arsenate increased $^{13}CO_2$ production by 10-fold, ultimately decreasing CH_4 emissions by 68.5%. The inhibition of CH_4 emissions by As was induced through three aspects: (1) the toxicity of As decreased the abundance and activity of the methanogens; (2) the adaptability and response of methanotrophs to As is beneficial for CH_4 oxidation under As stress; and (3) the more robust arsenate reduction would anaerobically consume more CH_4 in paddies. Additionally, significant positive correlations were observed between *arsC* and *pmoA* gene abundance in both the observational study and incubation experiment. These findings enhance our understanding of the mechanisms underlying the interactions between As and CH_4 cycling in soils.

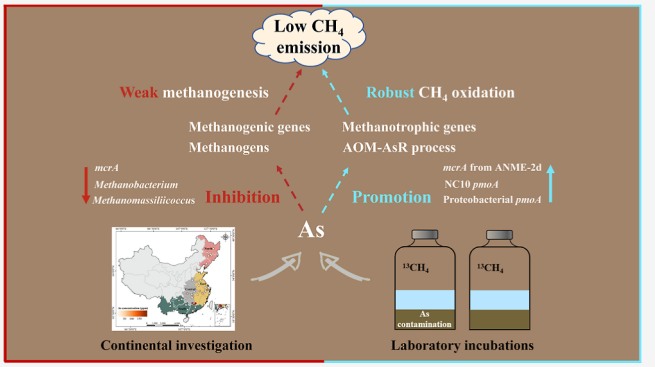

KEYWORDS: *arsenic, methanogenesis, CH_4 oxidation, CH_4 emission, arsenate reduction, paddy soils*

INTRODUCTION

Rice paddies are considered hot spots of methanogenesis, generating 25−37 Tg of methane (CH_4) per year (1 Tg = 10^{12} g), accounting for 11% of the total anthropogenic contribution to atmospheric CH_4.[1,2] Considerable studies have estimated the total amount of CH_4 emissions from rice fields in China, with values ranging from 2.26 to 21.62 Tg CH_4 per year.[3] The variation in CH_4 emissions' estimation could be attributed to climatic conditions, agricultural management practices, and soil heterogeneity.[4−6] Thus, the impact analysis of environmental factors on CH_4 cycling is highly important for quantifying emission inventories.

Among the critical soil properties impacting CH_4 fluxes, heavy metal(loid)s are unique. The anaerobic oxidation of CH_4 (AOM) driven by metal oxides (e.g., iron (Fe), manganese (Mn), and arsenic (As))[7,8] helps to reduce CH_4 emissions into the atmosphere. On the other hand, the toxicity of heavy metal(loid)s (e.g., cadmium (Cd) and nickel (Ni)) significantly inhibits CH_4 oxidation.[9] As is a redox-active contaminant ubiquitous in paddy fields. Naturally, widespread CH_4 was found to drive reductive As mobilization by coupling AOM to As(V) reduction (AOM-AsR), suggesting the great potential of coupled CH_4 and As metabolism.[8,10] However, the deeper connection among As(V) reduction, CH_4 production, and CH_4 oxidation processes needs further investigation.

In methanogenesis, methyl-coenzyme M reductase (MCR) catalyzes the terminal step of the pathway, while in AOM, MCR catalyzes the activation of CH_4.[11−13] Usually, the *mcrA* gene, which encodes the subunit alpha of the Mcr enzyme, is treated as a molecular marker of methanogenic archaea,[14] while specific *mcrA* genes from anaerobic methanotrophic archaea (ANME) are treated as molecular markers of AOM.[15,16] CH_4 monooxygenase, including particulate CH_4 monooxygenase (pMMO) and soluble CH_4 monooxygenase (sMMO), is the most critical enzyme in the CH_4 oxidation.[17] pMMO is found in nearly all methanotrophs, and thus the *pmoA* gene, encoding the β subunit of pMMO, and has become a well-established functional biomarker for detecting CH_4-oxidizing bacteria (MOB).[18,19] Although the respiratory

Received: July 5, 2024
Revised: September 6, 2024
Accepted: September 11, 2024
Published: September 24, 2024

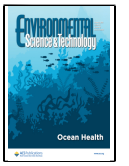

As(V) reductase gene (*arrA*) and ANME-*mcrA* gene were transcriptionally active in AOM-AsR, the correlations of the genes related to As reduction, CH_4 oxidation, and CH_4 production during a complete CH_4 cycle and As mobilization remain unclear.

To the best of our knowledge, linking CH_4-cycling microbiome dynamics of soil to the stress of As toxicity has rarely been achieved. No comprehensive study has been performed to elucidate how and to what extent As contamination alters CH_4 emissions and related genes on a continental scale. Therefore, we collected 132 soil samples from 44 rice paddies across continental China and conducted metagenome sequencing and reverse transcription polymerase chain reaction (RT-qPCR) to investigate the abundance and activity of CH_4-producing/-oxidizing and As-reducing microbes. The association between microbes involved in As and CH_4 metabolism, as deduced from metagenome analysis, was further validated through laboratory microcosm incubations. Our objectives were (1) to determine the effects of As on CH_4 emissions and (2) to reveal the potential microbial mechanisms underlying the impact of As on CH_4 emissions in paddies.

MATERIALS AND METHODS

Sample Collection. A total of 132 soil samples were obtained from 44 paddy fields extending from 22.51°N to 45.51°N and 102.88°E to 127.34°E throughout the main rice cropping areas in China. At each site, three samples were collected from the top 0−20 cm of the soil. Upon sampling, the soils were divided into two parts and transported to the laboratory immediately: one part was used for soil characterization analysis and incubation experiments, and the other was sealed in sterile valve bags, transported on dry ice, and then frozen at −80 °C until DNA and RNA extraction. We also collected some noncontaminated paddy soil samples for subsequent As-addition incubation experiments from one site located in Jiaxing (30°50′8.74″N, 120°43′3.68″E), Zhejiang, China. The physicochemical properties of these soil samples are listed in Supplementary Table S1.

Laboratory Incubation. Experiment 1: potential CH_4 emission rates and AOM rates in 15 representative paddy soils collected across China

Based on the soil physicochemical parameters, 15 representative paddies from 44 sampling sites were selected to cover different As levels and geographical areas for incubation experiments. The microcosm incubations were prepared as follows: approximately 25 g of dry soil was incubated in 125 mL serum bottles and 50 mL of sterile distilled deionized water. The headspace was further degassed by using pure argon (Ar) for 30 min to remove oxygen and immediately sealed with rubber stoppers and aluminum crimp seals. Finally, 5 mL of pure ^{13}C-labeled CH_4 was injected to maintain a $^{13}CH_4$ content of ∼10% (v/v) in the headspace. Each soil sample had one control experimental setup prepared without $^{13}CH_4$ (Ar groups). All other conditions were identical to those in the experimental setups. To avoid the interference of methanogenesis and other environmental factors, $^{13}CO_2$ within the headspace was obtained by subtracting the $^{13}CO_2$ values in the Ar treatment groups from those in the methane treatment groups, respectively. Each setup had four replicates. All the microcosms were incubated at 25 °C in a dark chamber, simulating the in situ conditions of paddy fields. The concentrations of CH_4, $^{13}CH_4$, and $^{13}CO_2$ in the headspace were measured every 7 days. The potential CH_4 emission rates were calculated by dividing the total amount of CH_4 produced in the argon groups by the total incubation time and were normalized to the soil dry weight. The potential AOM rates were calculated by dividing the total amount of $^{13}CO_2$ produced in the $^{13}CH_4$ groups by the total incubation time and were normalized to the soil dry weight (see Supporting Information for more details).

Experiment 2: dynamics of CH_4 production and oxidation in response to As stress

To assess the impact of As on soil CH_4 emissions, an aqueous solution of $Na_2HAsO_4{\cdot}7H_2O$ was applied to one uncontaminated soil located in Jiaxing (denoted ZJ-JX in Table S1) to achieve added As concentrations of 30 and 150 mg As kg^{-1} dry soil. These As-concentration levels are equivalent to slightly and highly As-contaminated agricultural land that need screening and intervention, respectively, according to the Risk Control Standards of China (GB15618-2018).[20] More details of the aging experiment can be found in the Supporting Information and previous studies.[21] After the contaminated soil was prepared, approximately 10 g of dry soil was incubated in 60 mL serum bottles along with 20 mL of Milli-Q water. Again, the medium was degassed to create anoxic conditions. All the bottles were tightly closed and sealed, half of which were followed by injecting 3.6 mL of ^{13}C-labeled CH_4 to a ratio of 10% (v/v) in the headspace. Three treatments were set up: (i) soil without As addition served as an experimental control (control); (ii) soil with 30 mg of As kg^{-1} soil As addition (low-As); and (iii) soil with 150 mg of As kg^{-1} soil As addition (high-As). The serum bottles were incubated at a constant temperature (25 ± 0.8 °C) under continuous dark conditions for 28 days. During different incubation periods (1, 7, 14, 21, and 28 d), the headspace gas composition was measured. Each treatment was replicated six times (three for the Ar treatment and three for the CH_4 treatment) and destructively sampled after incubation for 1, 14, and 28 days.

Chemical Analyses. The contents of heavy metals (i.e., As, Cd, chromium (Cr), lead (Pb), copper (Cu), and Ni) in the soil field samples were measured by inductively coupled plasma mass spectrometry (ICP−MS) (NexION300XX, PerkinElmer, Inc., USA) after digestion with a mixture of HNO_3, HF, and H_2O_2 (volume ratio = 4:2:2). Analytical blanks and the standard reference material GBW07405(soil) were also analyzed for quality control. The average recovery rates of As, Cd, Cr, Pb, Cu, and Ni were 97.8%, 96.1%, 93.3%, 92.9%, 98.9%, and 96.1%, respectively, in GBW07405. Porewater was sampled by centrifugation for 10 min at 3100*g* and acidification with 6 M HCl to prevent As transformation. Common As species (including As(III), As(V), DMA, and MMA) in porewater were measured by high-performance liquid chromatography (HPLC, PerkinElmer, Inc., USA) coupled to an ICP−MS instrument configured with an anion-exchange PRP X-100 HPLC column (250 × 4.1 mm I.D., Hamilton). Gaseous CH_4 and $^{13}CO_2$ were measured by an Agilent gas chromatography−mass spectrometer (GC−MS, GC 6890 N (G1530N), MS 5975B, injection volume: 10 μL) equipped with an HP-PLOT U column (19091P-UO4, ID: 30 m × 0.32 mm × 10 μm).

Nucleic Acid Extraction, Quantification, and Metagenomic Sequencing. Total DNA and RNA were extracted by Guangdong Magigene Biotechnology Co., Ltd. (Guangzhou, China) using an ALFA-SEQ Advanced Soil DNA Kit (Findrop, Guangzhou) and an RNeasy Mini Kit (Qiagen,

https://doi.org/10.1021/acs.est.4c06809
Environ. Sci. Technol. 2024, 58, 17685−17694

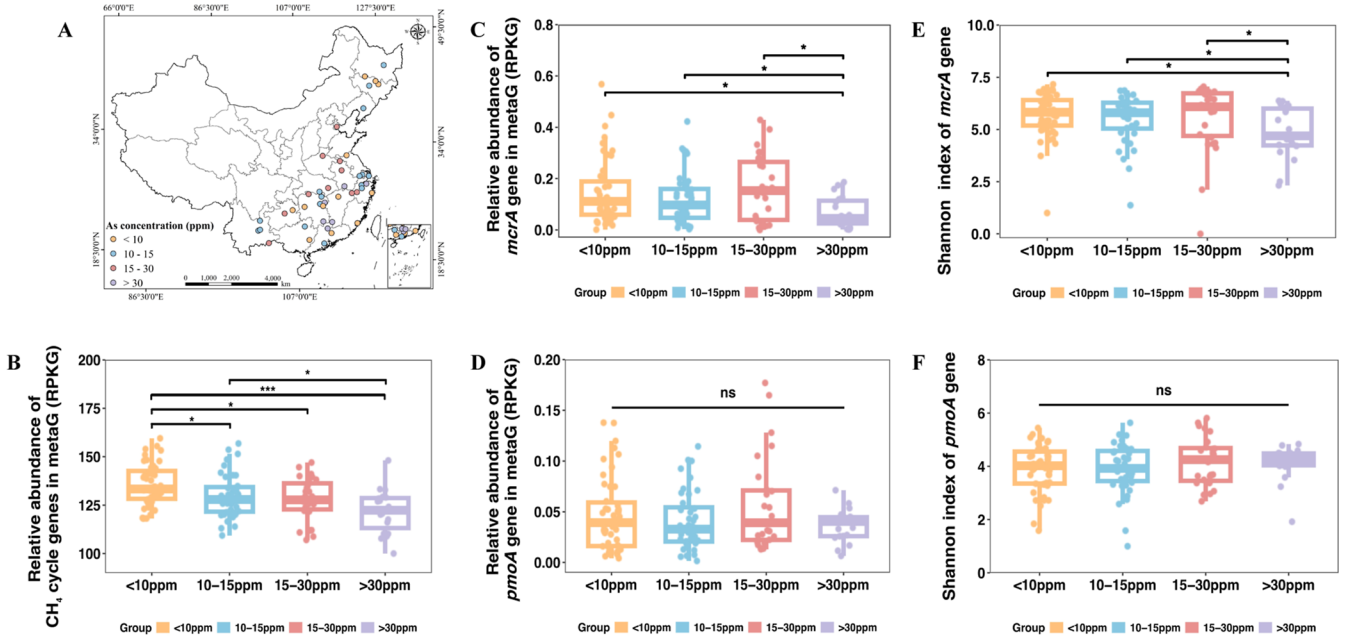

Figure 1. Geographic locations of sampling sites (A). Relative abundance of genes involved in CH_4 cycling (B), CH_4 production and anaerobic oxidation (*mcrA* gene) (C), and aerobic CH_4 oxidation (*pmoA* gene) (D). Alpha diversity (Shannon index) of the *mcrA* (E) and *pmoA* (F) genes. For all box plots in parts B–F, the lower and upper hinges correspond to the first and third quartiles, the upper and lower box plot whiskers represent the highest and lowest values within 1.5 times the interquartile range, and the horizontal line represents the median. Significance values for two-sided Wilcoxon rank-sum tests are denoted as follows: "ns" indicates not significant ($p > 0.05$), *$p < 0.05$, **$p < 0.01$, ***$p < 0.001$.

Germany), respectively, according to the manufacturer's instructions. More details of the soil DNA/RNA extraction can be found in the Supporting Information. DNA concentration and purity were measured using the NanoDrop One (Thermo Fisher Scientific, MA, USA). Soil DNA samples were subjected to shotgun metagenome sequencing in Shanghai Majorbio Bio-Pharm Technology Co., Ltd. and detailed in Supporting Information. The quality and concentration of the extracted RNA were assessed with a NanoDrop 2000 spectrophotometer (Thermo Fisher Scientific, Wilmington, DE, USA). The extracted RNA was reverse-transcribed to cDNA using the HiScript II first Strand cDNA Synthesis Kit and then used for quantitative PCR (qPCR) analysis using a Bioer Quant Gene 9600 Plus (FQD-96C, Hangzhou, China).

16S rRNA Gene High-Throughput Sequencing. To identify the changes in the functional microbial community in response to As contamination, a total of 52 DNA samples taken from the As-addition experiment at different incubation stages were analyzed for soil bacterial and archaeal communities through high-throughput sequencing on an Illumina Nova6000 platform of the 16S rRNA genes. The bacterial 16S rRNA genes (V3–V4 region) were amplified by the primers 338 F and 806 R.[22] The archaeal 16S rRNA genes (V4–V5 region) were amplified by the primers 519 F and 915 R.[23] All sequence data were deposited into the Nucleotide Archive database on the US National Center for Biotechnology Information (NCBI) Web site under PRJNA1092800. The sequencing procedure is detailed in the Supporting Information.

Functional Annotation of *arsC*, *arrA*, *mcrA*, and *pmoA* Genes in Metagenomic Data Sets. All the metagenomic sequencing data involved in the study have been submitted to the Sequence Read Archive with the BioProject accession number PRJNA1068274. The raw reads in 132 metagenomic data sets were trimmed of adaptors, and low-quality reads (length <50 bp or with a quality value <20) were removed by Multitrim (https://github.com/KGerhardt/multitrim). Clean reads were then used to estimate genome equivalents for each sample using MicrobeCensus v1.1.0. The read-based annotation of *arrA* and *arsC* genes was performed by blastx of diamond v2.0.14.152[24] against the self-constructed *arrA* database (detailed in Supporting Information) as well as the *arsC* database based on previous studies,[25] respectively, with an e-value cutoff of 1×10^{-5}, a minimum identity of 80%, and a minimum comparison length of 25 aa. Similarly, the *mcrA* and *pmoA* genes were annotated against the MCycDB with the same parameters.[26] Relative abundance of the gene was calculated as reads per kilobase per genome equivalents [RPKG = (reads mapped to gene)/(gene length in kb)/(genome equivalents)], which indicates the fraction of total cells encoding the gene of interest, i.e., copies per cell.[27]

Quantitative Polymerase Chain Reaction. 132 RNA samples obtained from continental collections were subjected to RT-qPCR analysis to quantify the transcript abundance of functional genes, including *mcrA* for methanogenesis, *pmoA* for CH_4 oxidation, and *arsC* for As(V) reduction. In addition, to study the dynamic changes in functional genes specifically, the following 54 DNA samples taken from the As-addition incubation experiment at d-1, d-14, and d-28 were also subjected to qPCR to quantify the abundance of archaeal *mcrA* (CH_4 production), ANME-*mcrA* (−1, −2a-c, −2d, and −3) (AOM), bacterial proteobacterial *pmoA* (CH_4 oxidation), NC10 *pmoA* (AOM), and *arrA* and *arsC* (As(V) reduction) genes. The details of the primer sequences, procedures, and systems used for qPCR amplification are shown in the Supporting Information.

Statistical Analyses. All the statistical analyses were performed in R (v4.3.1). Pearson's correlation analysis was performed to assess the correlations between two parameters.

https://doi.org/10.1021/acs.est.4c06809
Environ. Sci. Technol. 2024, 58, 17685−17694

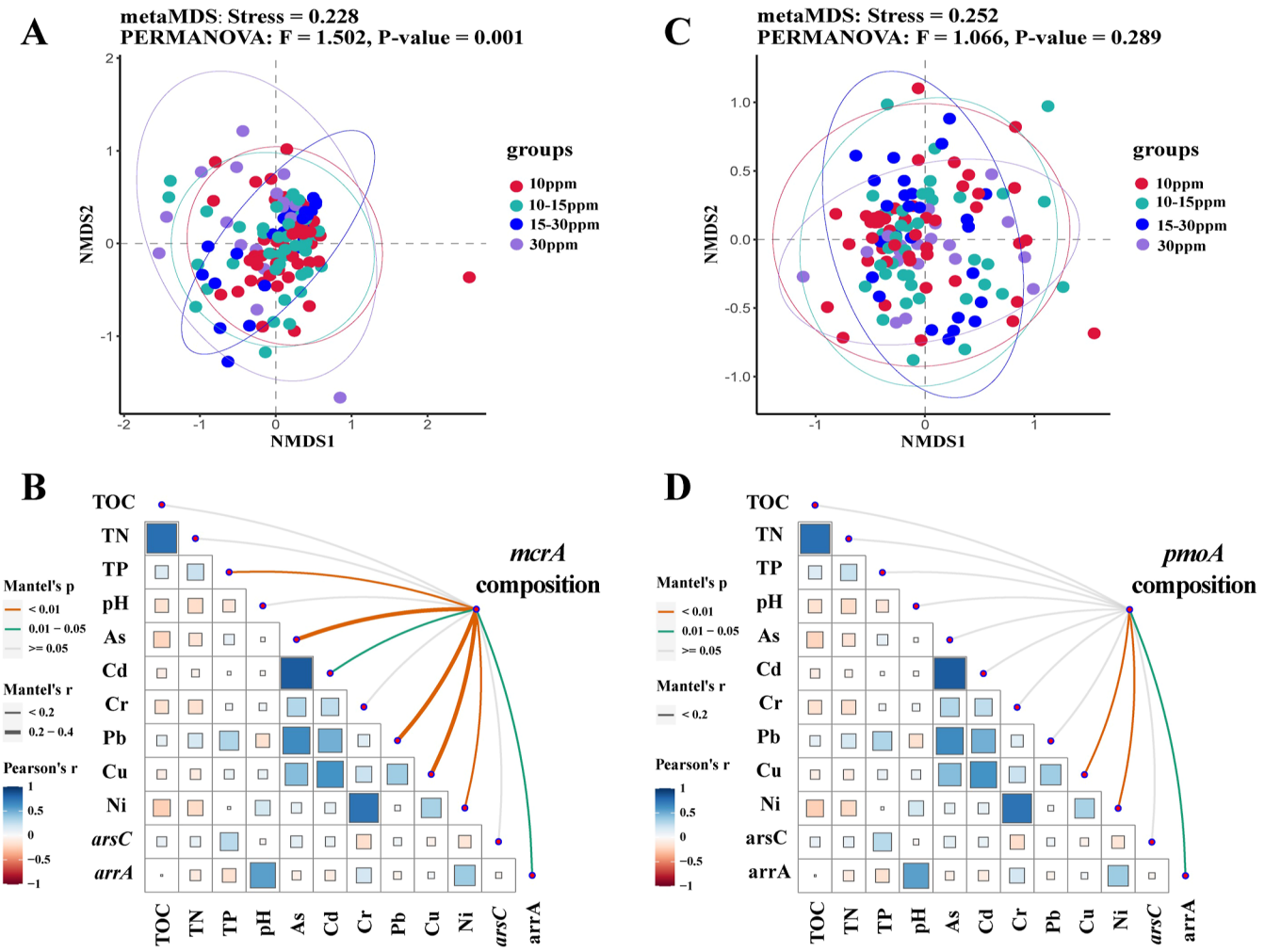

Figure 2. NMDS analysis of the *mcrA* gene (A) and the *pmoA* gene (C) across As gradients based on the Bray−Curtis taxonomic similarity. Correlations between the composition of the *mcrA* (B) and *pmoA* (D) genes and the soil properties, respectively. Edge width and color correspond to Mantel's *R* and *p* values, respectively. Pearson's correlations of the soil variables are shown with a color gradient.

A heatmap and Mantel test were constructed to disentangle potential environmental drivers of microbiome CH_4-cycling functions in paddy soils using the "ggcorrplot" and "linkET" packages, respectively. To compare the *mcrA* and *pmoA* microbial diversity, the Shannon indices of the annotated *mcrA* and *pmoA* genes were calculated by using the "vegan" package. The beta diversity of the *mcrA* and *pmoA* communities was assessed by Bray−Curtis similarity using the R packages "vegan" and "dplyr". Linear discriminant effect size (LEfSe) analysis was used to identify differentially abundant archaeal genera with As addition versus the control. Figures were prepared using Origin Pro 2018 (OriginLab) and R (v4.3.1) software.

RESULTS

Abundances and Diversity of *mcrA* and *pmoA* Genes along As Gradients at the Continental Scale in China. In total, 132 paddy soil samples were collected from Eastern, Central, and Southern China (Figure 1A). These samples were grouped into "low As," "low-medium As," "medium-high As," and "high As," according to the total As content, i.e., <10 ppm, 10−15 ppm, 15−30 ppm, and >30 ppm, respectively. A significantly higher relative abundance of CH_4-cycling genes was detected in the low As and low-medium As groups than in the medium-high As and high As groups ($p < 0.05$; Figure 1B). For microbially mediated anaerobic CH_4 production and oxidation, the lowest relative abundance of the *mcrA* gene annotated by metagenomic data sets was observed in the high As group, with significant differences relative to the other As groups (Figure 1C, $p < 0.05$). The α diversity of the *mcrA* gene, as represented by the Shannon diversity index, was also significantly lower in the high As group than in the other As groups (Figure 1E, $p < 0.05$). Nonmetric multidimensional scaling (NMDS) of the Bray−Curtis similarity of the *mcrA* genes demonstrated that microbial community compositions involved in CH_4 production and anaerobic CH_4 oxidation significantly varied among the low, low-medium, medium-high, and high As gradients (Figure 2A, $F = 0.152$, $p = 0.001$). For microbial communities involved in aerobic CH_4 oxidation, represented by the *pmoA* gene, no significant variation in the abundance, structure, or α diversity of the *pmoA* gene was detected among the four groups of As gradients (Figures 1D,F and 2C).

Factors Affecting the Community Compositions of the *mcrA* and *pmoA* Genes. Total As was the critical factor in explaining the variation in the structure of the microbes involved in anaerobic CH_4 production and oxidation, as revealed by Mantel tests of the correlation of *mcrA* gene

https://doi.org/10.1021/acs.est.4c06809
Environ. Sci. Technol. 2024, 58, 17685−17694

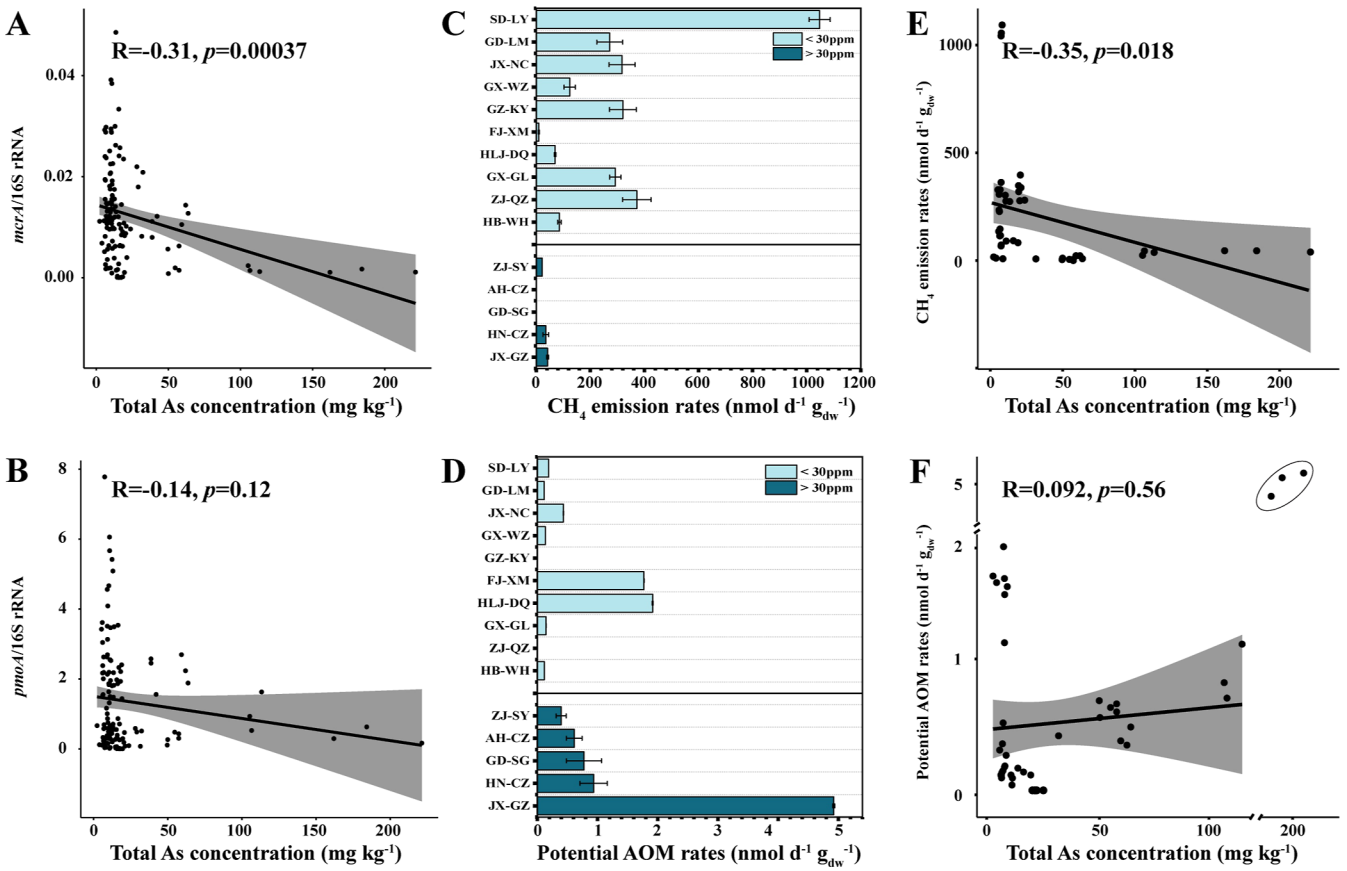

Figure 3. Linear relationships between the relative transcript abundance of the *mcrA* (A) or *pmoA* (B) genes and total As concentrations at the continental scale in China (132 samples). The transcription level of each gene was normalized to that of ambient 16S rRNA genes as the relative transcript abundance. Potential CH_4 emission rates (C) and potential AOM rates (D) in 15 representative paddy soils collected across China. The error bars indicate the standard deviations of quadruplicates. Linear relationships between potential CH_4 emission rates (E) and potential AOM rates (F) and total As concentration. Note: Due to the high As concentration and significant outliers at the three points in JX-GZ, these data were not included when comparing the correlations between potential AOM rates and As concentrations, as shown in Figure 3F.

composition with various soil properties (Figure 2B, $p < 0.01$). The total phosphorus, Pb, Cu, and Ni were also dominant factors (Figure 2B, $p < 0.01$) affecting the composition of the *mcrA* gene, followed by Cd ($p < 0.05$). The composition of the *pmoA* gene was not affected by surrounding environmental factors (including As content) except for Cu and Ni (Figure 2D). Notably, the community compositions of both the *mcrA* (Figure 2B, $p < 0.05$) and *pmoA* genes exhibited strong correlations with the relative abundance of As(V)-respiration-related *arrA* gene (Figure 2D, $p < 0.05$). Moreover, a significant ($p < 0.001$) and positive correlation was observed between the relative abundance of the *pmoA* and *arrA* genes, suggesting the coexistence of CH_4 oxidation and As(V) reduction functional genes in paddy soil microbial communities (Figure S2C).

Arsenic Gradients Affecting the Transcriptional Activities of Microbial Communities Involved in CH_4 Emissions. For the relative transcript abundance of the *mcrA* gene at the continental scale in China, a significant negative correlation was observed between the *mcrA* gene and the total As content (Figure 3A, $p < 0.001$). Consistently, the relative transcript abundance of the *mcrA* gene was significantly lower in the high As group than in the low As ($p < 0.0001$) and low-medium As ($p < 0.001$) groups, respectively (Figure S4A), suggesting that As inhibited *mcrA* gene expression. The relative transcript abundance of the *pmoA* gene was significantly lower in the medium-high As group than in the low As and low-medium As groups ($p < 0.05$), while there was no significant difference between the high As group and the other As groups (Figure S4B). Moreover, no significant ($p = 0.12$) correlation was found between the relative abundance of the reverse-transcribed *pmoA* gene and the As concentration (Figure 3B). Notably, the field-level correlations may be confounded by the complexity of the soils and the presence of multiple metal(loid)s, which are strongly correlated to each other (Figure S3), making it difficult to disentangle the causal variable.

Corroborative microcosm cultivation experiments of 15 representative paddy soils with different As contents, ranging from 4.9 to 189.1 mg kg^{-1}, further confirmed that the inhibition of CH_4 emission increased with increasing soil As content gradients. The CH_4 emission rates in the samples ranged from 0 to 1064.2 ± 26.3 nmol g^{-1} dry soil d^{-1} (Figure 3C). Specifically, the average emission rates of CH_4 in samples from the uncontaminated sites (<30 ppm) were greater than those at the As-contaminated sites (>30 ppm),[20] i.e., 291.6 *vs* 21.5 nmol g^{-1} dry soil d^{-1} (Figure S5A). The potential AOM rate was estimated by the generated $^{13}CO_2$ to evaluate the anaerobic CH_4 oxidation under different As concentrations. Considerable variances in the potential AOM rate were observed between soils with different As concentrations, ranging from 0 to 4.9 ± 0.02 nmol g^{-1} of dry soil d^{-1} (Figure

https://doi.org/10.1021/acs.est.4c06809
Environ. Sci. Technol. 2024, 58, 17685−17694

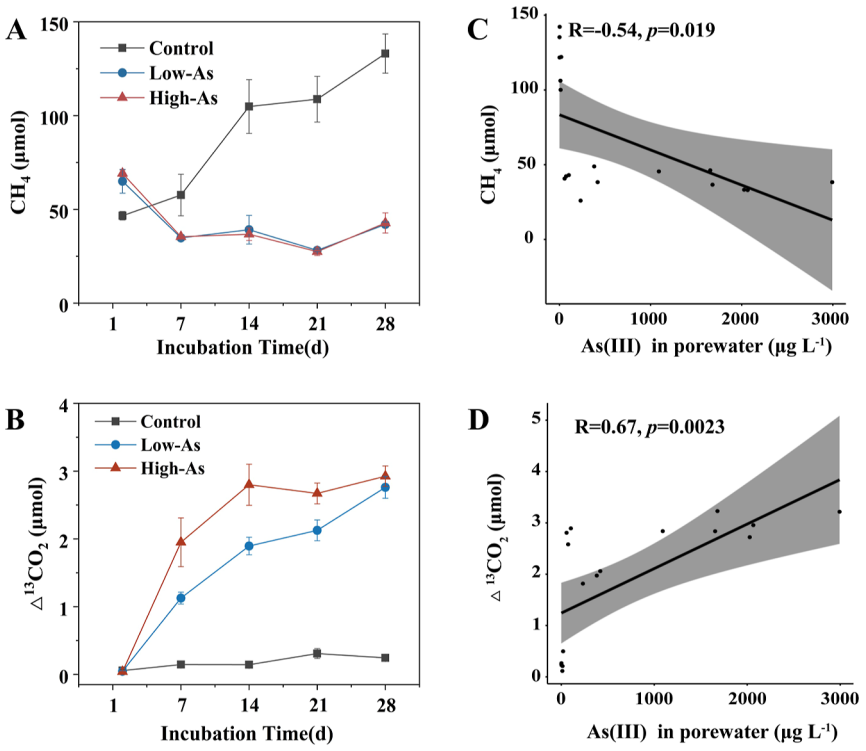

Figure 4. Dynamic changes in CH_4 (in Ar treatments) (A) and $\Delta^{13}CO_2$ (B) concentrations within the headspace of microcosms during the As-addition incubation experiment (control: soil without As addition; low-As: soil with 30 ppm As addition; high-As: soil with 150 ppm As addition). The linear relationships between the increased As(III) in soil porewater and the CH_4 (C) and $^{13}CO_2$ (D) generated within the headspace of microcosm incubations. Δ values indicate the difference between the experimental and control setups (in the presence or absence of $^{13}CH_4$). The error bars indicate the standard deviations of triplicate samples.

3D). The average AOM rates at the As-contaminated sites (>30 ppm) were higher than those at the uncontaminated sites (<30 ppm), i.e., 0.7 vs 0.4 nmol g^{-1} dry soil d^{-1} (Figure S5B). The total As in soils significantly affected the CH_4 emission rates and potential AOM rates (Figure S5); the CH_4 emission rates showed a decreasing trend with increasing As concentration ($R = -0.35$, $p = 0.018$; Figure 3E), while the potential AOM rates showed the opposite trend (Figure 3F).

Dynamics of CH_4 Production and Oxidation in Response to As Stress. Arsenic addition to the paddy soils inhibited CH_4 emissions, and the emission of CH_4 gradually decreased over time (Figure 4A). In the control microcosms without $^{13}CH_4$ injection, the CH_4 concentration increased to 133.1 μmol at the end of the incubation period. However, the CH_4 contents were only 42.0 and 42.8 μmol in the low-As and high-As groups, respectively (Figure 4A). Specifically, at the final incubation stage (28 days), As significantly reduced CH_4 emissions by 68.5% and 67.9%, respectively. ^{13}C tracing experiments were further carried out to estimate the effect of As on CH_4 oxidation to $^{13}CO_2$. After 28 days of incubation, the addition of 30 and 150 ppm As significantly increased the $^{13}CO_2$ concentration from 0.05 to 2.8 μmol and from 0.04 to 2.9 μmol, respectively (Figure 4B). However, the $^{13}CO_2$ content barely changed in the control group without As addition, with 0.2 μmol at the end of the incubation period (Figure 4B). During the 28 day incubation, As(V) was significantly reduced to As(III). The highest As(III) concentration was observed on day 14, with values of 14.78 ± 4.29 μg L^{-1}, 400.49 ± 26.79 μg L^{-1}, and 2046.12 ± 27.27 μg L^{-1} in soil porewater in the control, low-As, and high-As groups, respectively (Figure S6A). The increased dissolved As(III) in porewater was positively correlated with the $\Delta^{13}CO_2$ concentration (Figure 4D) ($R = 0.67$, $p < 0.01$), obtained by $^{13}CH_4$ treatments subtracting the amount in the Ar treatments, while negatively correlated with CH_4 concentration generated in the headspace of the Ar treatments (Figure 4C) ($R = -0.54$, $p < 0.05$).

The relative abundances of key functional genes were quantified by normalization of the absolute gene copy numbers to those of the ambient 16S rRNA gene during the incubation. For genes involved in CH_4 oxidation, the addition of 30 ppm As increased the relative abundance of the ANME-2d *mcrA*, *pmoA*, and NC10 *pmoA* genes by 93.1%, 111.7%, and 158.7%, respectively, on day 14 compared to the control. These effects were also observed in the presence of 150 ppm of As (Figure 5A). In contrast, for genes involved in CH_4 production, the relative abundance of the *mcrA* gene decreased significantly from $1.11 \times 10^{0} \pm 3.09 \times 10^{-1}$ to $2.29 \times 10^{-1} \pm 2.94 \times 10^{-2}$ and $2.65 \times 10^{-1} \pm 5.76 \times 10^{-2}$ with 30 and 150 ppm As addition, respectively, on day 14 (Figure 5A, $p < 0.001$). At the end of the 28 day incubation, the abundance of all these genes decreased in all of the treatment groups (Figure S7). A significant positive correlation between the *arrA* and *pmoA* genes was revealed in the low-As and high-As groups on day 14 (Figure 5E,F, $p < 0.001$), while this correlation was not detected in the control group (Figure 5D). Moreover, the relative abundance of the *arsC* and *pmoA* genes showed a significantly positive correlation in the high-As group on day 14 (Figure 5F, $p < 0.001$). Based on 16S rRNA gene high-throughput sequencing, the alpha diversity of total bacteria and archaea was reduced by As addition in the paddy soils (Tables S4 and S5). Furthermore, using LEfSe analysis, we found that

https://doi.org/10.1021/acs.est.4c06809
Environ. Sci. Technol. 2024, 58, 17685−17694

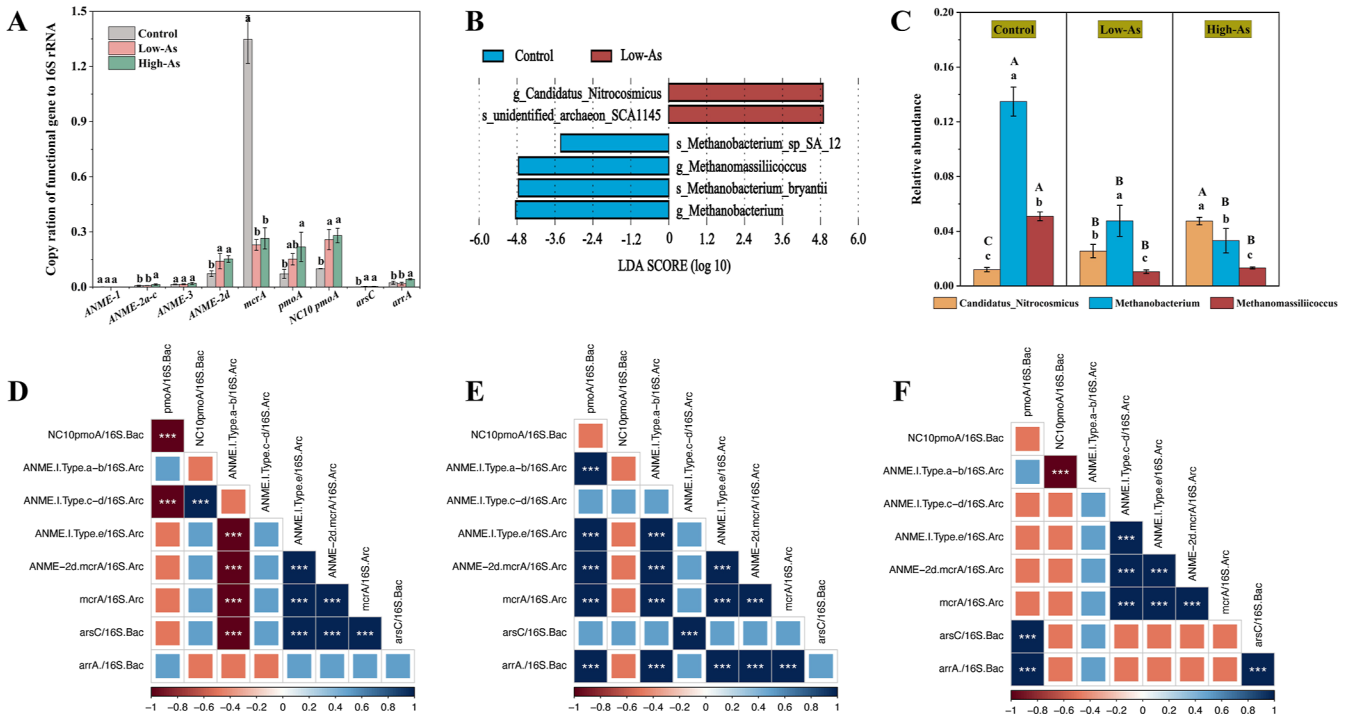

Figure 5. Effect of As on the relative abundance of the *mcrA*, ANME-*mcrA* (−1, −2a-c, −2d, and −3), *pmoA*, NC10 *pmoA*, *arsC*, and *arrA* genes (A) in the As-addition incubation experiment on day 14. LEfSe analysis of the differentially abundant archaeal genera in the As treatment group versus the control group (B). Relative abundance of the differential archaeal genera on day 14 (C). Correlations between the relative abundances of functional genes in the As-addition incubation experiment. (D−F) represent the samples from the control, low-As, and high-As groups after 14 days, respectively (control: soil without As addition; low-As: soil with 30 ppm As addition; high-As: soil with 150 ppm As addition). *P*-value significance levels were corrected using the Benjamini−Hochberg method for multiple testing and denoted as $*p < 0.05$, $**p < 0.01$, and $***p < 0.001$. The error bars indicate the standard deviations of triplicate samples. The different lowercase letters in (A) indicate significant differences ($p < 0.05$) among the different treatments on day 14. The different lowercase letters in (C) indicate significant differences ($p < 0.05$) among the three archaeal genera in the same treatment, whereas the different capital letters indicate significant differences ($p < 0.05$) for the same genus among the different treatments on day 14.

the relative abundance of *Methanomassiliicoccus* and *Methanobacterium* in the low-As group (1.1% and 4.8%) was significantly lower than that in the control group (5.1% and 13.5%), whereas the *Candidatus_Nitrocosmicus* was higher (2.6%) than that in the control (1.2%) on day 14 ($p < 0.05$; Figure 5B,C). Compared to the control group, 30 ppm As addition decreased the abundance of *Methanomassiliicoccus* and *Methanobacterium* by 79.3% and 75.4%, respectively, on day 14 and by 98.4% and 89.7%, respectively, on day 28 (Figures 5C and S9B). These differences were also significant ($p < 0.001$) between the high-As and control groups (Figures 5C and S9B).

DISCUSSION

Direct Inhibition of CH_4 Production by As Stress. Soils with high As contamination levels are usually characterized by low soil enzyme activities, low carbon mineralization, and low nitrification potential.[28] Previous studies suggested that the abundance of *mcrA* genes was positively correlated with total As content in high As groundwater.[29] However, our study comprehensively confirmed that methanogenesis, governed by *mcrA*-harboring microorganisms, was inhibited in As-contaminated soils (Figures 1C,E, 2B, and 3A). Compared to abiotic CH_4 emissions (e.g., from fossil fuels), there is a high degree of uncertainty associated with microbially mediated CH_4 emissions, and different environmental factors can significantly affect methanogenic communities.[30] Of the soil properties considered in previous studies, pH was suggested to be the limiting factor for the growth of methanogens and their richness.[31] In the present study, considering that most paddy soils were weakly acidic and neutral (Table S1, ranging from 4.48 to 8.02), close to the optimum pH range for methanogens,[32] no significant correlation of soil pH with the abundance or structure of the methanogenic *mcrA* gene ($p > 0.05$, Figures S1, 2B, S3) was detected. Furthermore, we expected that As(III) would have been less adsorbed on soil mineral surfaces than As(V) under these pH conditions based on high As(V) adsorption to iron oxide surfaces at weakly acidic to circumneutral pH and thus had greater biological availability and toxicity to microbes.[33] As previously reported, the inhibitory effect of As on *mcrA* genes and methanogenic archaea was likely due to its toxicity to acetate-utilizing methanogens. The highly toxic As(III) species accumulated from the reductive biotransformation of As(V) in anaerobic environments could seriously impact methanogenesis.[34,35] The results of the laboratory microcosm incubations further confirmed that the increased As(III) concentration from As(V) reduction was significantly and negatively correlated with CH_4 generated within the headspace (Figure 4C) ($p < 0.05$). Consistent with the large-scale sequencing analyses, the relative abundance of the *mcrA* gene, as well as that of the dominant methanogenic archaea *Methanobacterium* and *Methanomassiliicoccus*, decreased significantly with increasing concentrations of As in the paddy soils (Figure 5A−C). Interestingly, the prevalence of As contamination across continental rice paddies was closely correlated with intricate

https://doi.org/10.1021/acs.est.4c06809
Environ. Sci. Technol. 2024, 58, 17685−17694

methanogenesis, considering that the As content was significantly correlated with the abundance of the *mcr* gene cluster (*mcrABCDG*) encoding the coenzyme Mcr, which is involved in the last but core rate-limiting step of methanogenesis (Figure S1).[14] We also found that the keystone taxa involved in CH_4 cycling were strongly related to As concentrations, and the dominant MCR-containing groups of *Methanosarcinales* and *Methanomicrobiales* decreased along As gradients (metatranscriptomics approaches) (Figure S10).

Stimulatory Effect of As on CH_4 Oxidation. In the present study, 30 ppm As addition significantly increased the transformation of $^{13}CH_4$ to $^{13}CO_2$ 10-fold (Figure 4B). The CH_4 oxidation potential in soils is regulated mainly by methanotroph abundance and community activity.[36] The *pmoA* gene is widely used as a biomarker to detect methanotrophic communities.[19] Unlike the repression of the *mcrA* gene by As, the relative abundance, diversity, and activity of the *pmoA* gene in the As-contaminated sites (>30 ppm) were comparable to those in the uncontaminated sites (<10 ppm) (Figures 1D,F and S4B). Additionally, the composition of *pmoA* was not affected by the As content (Figure 2D). Severe As contamination may cause selection pressure to enrich microbes adapted to harsh environments.[37] The adaptability and response of methanotrophs to As contamination are beneficial for the CH_4 oxidation under As stress.

CH_4 oxidation coupled to As(V) reduction may be widespread in paddies, supported by the simultaneous presence of *arrA* and *pmoA* genes sampled from various natural paddies (Figure S2C) ($p < 0.001$), which is consistent with the findings of a previous study.[38] Microbes utilize As(V) as an electron acceptor for anaerobic respiration via the dissimilatory pathway mediated by the *arrA* and *arrB* genes,[39] while the cytoplasmic pathway involves the reduction of As(V) to As(III) by the *arsC* gene-encoded As(V) reductase followed by extrusion from the cell.[40] Interestingly, the relative transcript abundance of the *pmoA* gene also showed a significantly positive correlation with that of the *arsC* gene at the continental scale in China (Figure S4E, $R = 0.5$, $p < 0.001$). Consistently, a strong positive correlation between *arsC* and *pmoA* genes was further observed in the microcosm incubations with As addition (Figure S8), indicating the potential role of *arsC*-carrying microbes in CH_4 cycling in soils. Moreover, the ANME-*mcrA*, *pmoA*, and NC10 *pmoA* genes responsible for CH_4 oxidation were also observed to have greater relative abundances in paddy soils with 30 ppm of As than in the control treatment, implying the potential promotion of CH_4 oxidation by As (Figure 5A).

Furthermore, paddy soil with a higher As content possessed more substantial reductive dissolution of As-bearing iron minerals under continuously flooded conditions,[41] which could increase the availability of As(V) as an electron acceptor and thus possibly facilitate CH_4 oxidation. The microcosm incubation experiment confirmed that the addition of As(V) (30 and 150 ppm) increased the CH_4-driven pathway to As transfer (Figure S6), which in turn contributed to the more robust AOM efficiency in As-contaminated paddies (Figure 4B,D). Additionally, the availability of electron acceptors had a strong selective effect on ANMEs and the oxidation of CH_4.[42] A high concentration of As(V) enhanced the competition of As(V) for CH_4 oxidation, leading to the more robust AOM-AsR process in As-contaminated paddies. Thus, the stimulatory effect of As on CH_4 oxidation was induced from two effects: (1) the adaptability and detoxification ability of methanotrophs experiencing As stress and (2) the anaerobic CH_4 oxidation coupled to As(V) reduction which led to more robust CH_4 oxidation in As-contaminated soils.

In conclusion, based on an observational study across China and two laboratory validations, our findings highlight the importance of As in paddy soils as an environmental factor impacting CH_4-related microbial community abundance, activity, and diversity. High As toxicity in flooded paddies resulted in low activity and biomass of methanogens and decreased CH_4 emissions. Notably, the continental distribution of methanotrophs and their adaptation to high As concentrations may suggest the substantial role of this microbial group in the CH_4 cycling of As-contaminated paddy soils. Moreover, stronger As(V) reduction would occur in heavily As-contaminated paddies and anaerobically consume more CH_4, demonstrating AOM-AsR as an important CH_4 sink in heavily As-contaminated sites, probably regulating biogeochemical CH_4 cycling. This study provides valuable insights into the complex relationship between As biogeochemistry and CH_4 dynamics, contributing to the addition and correction of environmental parameters in the mechanism model of CH_4 emissions. Additionally, more careful strategies are required when dealing with As-contaminated soil in the case of As-induced CH_4 imbalance.

■ ASSOCIATED CONTENT

Data Availability Statement

Data and codes are available from the corresponding author upon request.

Supporting Information

The Supporting Information is available free of charge at https://pubs.acs.org/doi/10.1021/acs.est.4c06809.

Preparation of As-contaminated soils; calculation methods of the rates of $^{13}CO_2$ and CH_4 generation; details regarding qPCR of genes, 16S rRNA sequencing, metagenomic sequencing, metatranscriptomic sequencing, and data analysis; physicochemical characteristics of collected soil samples; correlations between the relative abundances of the *mcrA*, *pmoA*, *arsC*, and *arrA* genes and between functional genes and edaphic properties; alpha diversity of bacterial and archaeal communities and relative abundances of the functional genes and the main bacterial and archaeal genus during the As-addition incubation experiment; arsenic species in porewater during the As-addition incubation experiment; and relative abundance of the potentially active populations based on metatranscriptomics (PDF)

■ AUTHOR INFORMATION

Corresponding Author

Xian-Jin Tang − *Institute of Soil and Water Resources and Environmental Science, College of Environmental and Resource Sciences, Zhejiang Provincial Key Laboratory of Agricultural Resources and Environment, Zhejiang University, Hangzhou 310058, China;* orcid.org/0000-0002-7515-2047; Phone: +86-571-88982483; Email: xianjin@zju.edu.cn; Fax: +86-571-88981358

Authors

Ou-Yuan Jiang − *Institute of Soil and Water Resources and Environmental Science, College of Environmental and Resource Sciences, Zhejiang Provincial Key Laboratory of*

https://doi.org/10.1021/acs.est.4c06809
Environ. Sci. Technol. 2024, 58, 17685−17694

Agricultural Resources and Environment, Zhejiang University, Hangzhou 310058, China

Si-Yu Zhang − *School of Ecological and Environmental Sciences, East China Normal University, Shanghai 200241, China;* orcid.org/0000-0001-6701-5790

Xin-Di Zhao − *School of Ecological and Environmental Sciences, East China Normal University, Shanghai 200241, China*

Zi-Teng Liu − *School of Ecological and Environmental Sciences, East China Normal University, Shanghai 200241, China;* orcid.org/0000-0002-3583-4238

Andreas Kappler − *Department of Geosciences, University of Tübingen, Tübingen 72076, Germany;* orcid.org/0000-0002-3558-9500

Jian-Ming Xu − *Institute of Soil and Water Resources and Environmental Science, College of Environmental and Resource Sciences, Zhejiang Provincial Key Laboratory of Agricultural Resources and Environment, Zhejiang University, Hangzhou 310058, China;* orcid.org/0000-0002-2954-9764

Complete contact information is available at: https://pubs.acs.org/10.1021/acs.est.4c06809

Author Contributions

‖O.-Y.J. and S.-Y.Z. contributed equally to this paper.

Notes

The authors declare no competing financial interest.

■ ACKNOWLEDGMENTS

This work was financially supported by the National Natural Science Foundation of China (grant numbers 42122048, 42107135, and 41991332).

■ REFERENCES

(1) Canadell, J. G.; Monteiro, P. M. S.; Costa, M. H.; Cotrim da Cunha, L.; Cox, P. M.; Eliseev, A. V.; Henson, S.; Ishii, M.; Jaccard, S.; Koven, C.; Lohila, A.; Patra, P. K.; Piao, S.; Rogelj, J.; Syampungani, S.; Zaehle, S.; Zickfeld, K. 2021: Global Carbon and other Biogeochemical Cycles and Feedbacks. In *Climate Change 2021: The Physical Science Basis. Contribution of Working Group I to the Sixth Assessment Report of the Intergovernmental Panel on Climate Change*; Cambridge University Press: Cambridge, United Kingdom and New York, NY, USA, 2023; pp 673−816.

(2) Scholz, V. V.; Meckenstock, R. U.; Nielsen, L. P.; Risgaard-Petersen, N. Cable bacteria reduce methane emissions from rice-vegetated soils. *Nat. Commun.* **2020**, *11* (1), 1878.

(3) Wang, Z.; Zhang, X. Y.; Liu, L.; Wang, S. Q.; Zhao, L. M.; Wu, X. D.; Zhang, W. T.; Huang, X. J. Estimates of methane emissions from Chinese rice fields using the DNDC model. *Agric. For. Meteorol.* **2021**, *303*, 108368.

(4) Khalil, M. A. K.; Rasmussen, R. A.; Shearer, M. J.; Dalluge, R. W.; Ren, L.; Duan, C. Factors affecting methane emissions from rice fields. *J. Geophys. Res. Atmos.* **1998**, *103*, 25219−25231.

(5) Huang, Y.; Jiao, Y.; Zong, L. G.; Zheng, X. H.; Sass, R. L.; Fisher, F. M. Quantitative dependence of methane emission on soil properties. *Nutr. Cycling Agroecosyst.* **2002**, *64* (1/2), 157−167.

(6) Sass, R. L.; Fisher, F. M.; Wang, Y. B.; Turner, F. T.; Jund, M. F. Methane emission from rice fields: the effect of floodwater management. *Global Biogeochem. Cycles* **1992**, *6*, 249−262.

(7) Beal, E. J.; House, C. H.; Orphan, V. J. Manganese-and iron-dependent marine methane oxidation. *Science* **2009**, *325*, 184−187.

(8) Shi, L. D.; Guo, T.; Lv, P. L.; Niu, Z. F.; Zhou, Y. J.; Tang, X. J.; Zheng, P.; Zhu, L. Z.; Zhu, Y. G.; Kappler, A.; Zhao, H. P. Coupled anaerobic methane oxidation and reductive arsenic mobilization in wetland soils. *Nat. Geosci.* **2020**, *13*, 799−805.

(9) Wissink, M.; Glodowska, M.; van der Kolk, M. R.; Jetten, M. S. M.; Welte, C. U. Probing denitrifying anaerobic methane oxidation via antimicrobial intervention: implications for innovative wastewater management. *Environ. Sci. Technol.* **2024**, *58* (14), 6250−6257.

(10) Glodowska, M.; Stopelli, E.; Schneider, M.; Rathi, B.; Straub, D.; Lightfoot, A.; Kipfer, R.; Berg, M.; Jetten, M.; Kleindienst, S.; Kappler, A.; et al. Arsenic mobilization by anaerobic iron-dependent methane oxidation. *Commun. Earth Environ.* **2020**, *1* (1), 42.

(11) Krüger, M.; Meyerdierks, A.; Glöckner, F. O.; Amann, R.; Widdel, F.; Kube, M.; Reinhardt, R.; Kahnt, J.; Böcher, R.; Thauer, R. K.; Shima, S. A conspicuous nickel protein in microbial mats that oxidize methane anaerobically. *Nature* **2003**, *426* (6968), 878−881.

(12) Hallam, S. J.; Girguis, P. R.; Preston, C. M.; Richardson, P. M.; Delong, E. F. Identification of methyl coenzyme M reductase A (mcrA) genes associated with methane-oxidizing archaea. *Appl. Environ. Microbiol.* **2003**, *69* (9), 5483−5491.

(13) Hallam, S. J.; Putnam, N.; Preston, C. M.; Detter, J. C.; Rokhsar, D.; Richardson, P. M.; DeLong, E. F. Reverse methanogenesis: testing the hypothesis with environmental genomics. *Science* **2004**, *305* (5689), 1457−1462.

(14) Scheller, S.; Goenrich, M.; Boecher, R.; Thauer, R. K.; Jaun, B. The key nickel enzyme of methanogenesis catalyses the anaerobic oxidation of methane. *Nature* **2010**, *465* (7298), 606−608.

(15) Nunoura, T.; Oida, H.; Toki, T.; Ashi, J.; Takai, K.; Horikoshi, K. Quantification of mcrA by quantitative fluorescent PCR in sediments from methane seep of the Nankai Trough. *FEMS Microbiol. Ecol.* **2006**, *57* (1), 149−157.

(16) Vaksmaa, A.; Jetten, M. S. M.; Ettwig, K. F.; Lüke, C. McrA primers for the detection and quantification of the anaerobic archaeal methanotroph 'Candidatus Methanoperedens nitroreducens'. *Appl. Microbiol. Biotechnol.* **2017**, *101* (4), 1631−1641.

(17) Sirajuddin, S.; Rosenzweig, A. C. Enzymatic oxidation of methane. *Biochemistry* **2015**, *54* (14), 2283−2294.

(18) Mcdonald, I. R.; Bodrossy, L.; Chen, Y.; Murrell, J. C. Molecular ecology techniques for the study of aerobic methanotrophs. *Appl. Environ. Microbiol.* **2008**, *74* (5), 1305−1315.

(19) Knief, C. Diversity and habitat preferences of cultivated and uncultivated aerobic methanotrophic bacteria evaluated based on *pmoA* as molecular marker. *Front. Microbiol.* **2015**, *6*, 1346.

(20) Ministry of Ecology and Environment of the People's Republic of China. Soil environmental quality risk control standard for soil contamination of agricultural land (GB15618-2018). 2024, https://www.mee.gov.cn (accessed Feb 17, 2024).

(21) Zhao, H. C.; Yu, L.; Yu, M. J.; Afzal, M.; Dai, Z. M.; Brookes, P.; Xu, J. M. Nitrogen combined with biochar changed the feedback mechanism between soil nitrification and Cd availability in an acidic soil. *J. Hazard. Mater.* **2020**, *390*, 121631.

(22) Caporaso, J. G.; Lauber, C. L.; Walters, W. A.; Berg-Lyons, D.; Lozupone, C. A.; Turnbaugh, P. J.; Fierer, N.; Knight, R. Global patterns of 16S rRNA diversity at a depth of millions of sequences per sample. *Proc. Natl. Acad. Sci. U.S.A.* **2011**, *108*, 4516−4522.

(23) Coolen, M. J. L.; Hopmans, E. C.; Rijpstra, W. I. C.; Muyzer, G.; Schouten, S.; Volkman, J. K.; Sinninghe Damsté, J. S. Evolution of the methane cycle in Ace Lake (Antarctica) during the Holocene: response of methanogens and methanotrophs to environmental change. *Org. Geochem.* **2004**, *35* (10), 1151−1167.

(24) Buchfink, B.; Xie, C.; Huson, D. H. Fast and sensitive protein alignment using diamond. *Nat. Methods* **2015**, *12* (1), 59−60.

(25) Chen, S.; Sun, G. X.; Yan, Y.; Konstantinidis, K. T.; Zhang, S. Y.; Deng, Y.; Li, X. M.; Cui, H. L.; Musat, F.; Popp, D.; Rosen, B. P.; Zhu, Y. G. The great oxidation event expanded the genetic repertoire of arsenic metabolism and cycling. *Proc. Natl. Acad. Sci. U.S.A.* **2020**, *117* (19), 10414−10421.

(26) Qian, L.; Yu, X. L.; Zhou, J. Y.; Gu, H.; Ding, J. J.; Peng, Y. S.; He, Q.; Tian, Y.; Liu, J. H.; Wang, S. Q.; Wang, C.; Shu, L. F.; Yan, Q. Y.; He, J. G.; Liu, G. L.; Tu, Q. C.; He, Z. L. MCycDB: a curated database for comprehensively profiling methane cycling processes of environmental microbiomes. *Mol. Ecol. Resour.* **2022**, *22* (5), 1803−1823.

(27) Zhang, S. Y.; Xiao, X.; Chen, S. C.; Zhu, Y. G.; Sun, G. X.; Konstantinidis, K. T. High arsenic levels increase activity rather than diversity or abundance of arsenic metabolism genes in paddy soils. *Appl. Environ. Microbiol.* **2021**, *87* (20), No. e0138321.
(28) Yu, H.; Zheng, X. F.; Weng, W. L.; Yan, X. Z.; Chen, P. B.; Liu, X. Y.; Peng, T.; Zhong, Q. P.; Xu, K.; Wang, C.; Shu, L. F.; Yang, T.; Xiao, F. S.; He, Z. L.; Yan, Q. Y. Synergistic effects of antimony and arsenic contaminations on bacterial, archaeal and fungal communities in the rhizosphere of miscanthus sinensis: Insights for nitrification and carbon mineralization. *J. Hazard. Mater.* **2021**, *411*, 125094.
(29) Wang, Y. H.; Li, P.; Dai, X. Y.; Zhang, R.; Jiang, Z.; Jiang, D. W.; Wang, Y. X. Abundance and diversity of methanogens: Potential role in high arsenic groundwater in Hetao Plain of Inner Mongolia, China. *Sci. Total Environ.* **2015**, *515*−*516*, 153−161.
(30) Schaefer, H.; Fletcher, S. E. M.; Veidt, C.; Lassey, K. R.; Brailsford, G. W.; Bromley, T. M.; Dlugokencky, E. J.; Michel, S. E.; Miller, J. B.; Levin, I.; Lowe, D. C.; Martin, R. J.; Vaughn, B. H.; White, J. W. C. A 21st-century shift from fossil-fuel to biogenic methane emissions indicated by $^{13}CH_4$. *Science* **2016**, *352* (6281), 80−84.
(31) Ye, R.; Jin, Q. S.; Brendan, B.; Jason, K. K.; Steven, A. M.; Scott, D. B. pH controls over anaerobic carbon mineralization, the efficiency of methane production, and methanogenic pathways in peatlands across an ombrotrophic-minerotrophic gradient. *Soil Biol. Biochem.* **2012**, *54*, 36−47.
(32) Dunfield, P.; Knowles, R.; Dumont, R.; Moore, T. Methane production and consumption in temperate and subarctic peat soils: response to temperature and pH. *Soil Biol. Biochem.* **1993**, *25*, 321−326.
(33) Goldberg, S. Competitive adsorption of arsenate and arsenite on oxides and clay minerals. *Soil Sci. Soc. Am. J.* **2002**, *66* (2), 413−421.
(34) Sierra-Alvarez, R.; Cortinas, I.; Yenal, U.; Field, J. A. Methanogenic inhibition by arsenic compounds. *Appl. Environ. Microbiol.* **2004**, *70* (9), 5688−5691.
(35) Rodriguez-Freire, L.; Moore, S. E.; Sierra-Alvarez, R.; Field, J. A. Adaptation of a methanogenic consortium to arsenite inhibition. *Water, Air, Soil Pollut.* **2015**, *226* (12), 414.
(36) Tate, K. R. Soil methane oxidation and land-use change—from process to mitigation. *Soil Biol. Biochem.* **2015**, *80*, 260−272.
(37) Sun, W. M.; Xiao, E. Z.; Xiao, T. F.; Krumins, V.; Wang, Q.; Häggblom, M.; Dong, Y. R.; Tang, S.; Hu, M.; Li, B. Q.; Xia, B. Q.; Liu, W. Response of soil microbial communities to elevated antimony and arsenic contamination indicates the relationship between the innate microbiota and contaminant fractions. *Environ. Sci. Technol.* **2017**, *51* (16), 9165−9175.
(38) Shi, L. D.; Zhou, Y. J.; Tang, X. J.; Kappler, A.; Chistoserdova, L.; Zhu, L. Z.; Zhao, H. P. Coupled Aerobic methane oxidation and arsenate reduction contributes to soil-arsenic mobilization in agricultural fields. *Environ. Sci. Technol.* **2022**, *56* (16), 11845−11856.
(39) Malasarn, D.; Saltikov, W.; Campbell, K. M.; Santini, J. M.; Hering, J. G.; Newman, D. K. *arrA* is a reliable marker for As(V) respiration. *Science* **2004**, *306* (5695), 455.
(40) Carlin, A.; Shi, W.; Dey, S.; Rosen, B. P. The ars operon of Escherichia coli confers arsenical and antimonial resistance. *J. Bacteriol.* **1995**, *177*, 981.
(41) Borch, T.; Kretzschmar, R.; Kappler, A.; Cappellen, P. V.; Ginder-Vogel, M.; Voegelin, A.; Campbell, K. Biogeochemical redox processes and their impact on contaminant dynamics. *Environ. Sci. Technol.* **2010**, *44* (1), 15−23.
(42) Schnakenberg, A.; Aromokeye, D. A.; Kulkarni, A.; Maier, L.; Wunder, L. C.; Richter, H. T.; Pape, T.; Ristova, P. P.; Bühring, S. I.; Dohrmann, I.; Bohrmann, G.; Kasten, S.; Friedrich, M. W. Electron acceptor availability shapes anaerobically methane oxidizing archaea (ANME) communities in South Georgia sediments. *Front. Microbiol.* **2021**, *12*, 617280.

https://doi.org/10.1021/acs.est.4c06809
Environ. Sci. Technol. 2024, 58, 17685−17694